Tetrahedron 66 (2010) 9165–9170

Contents lists available at ScienceDirect

Tetrahedron

journal homepage: www.elsevier.com/locate/tet

Base dependent pyrrolidine ring pucker in *aep*-PNA monomers: NMR and PSEUROT analysis

Nagendra K. Sharma [a,*], Krishna N. Ganesh [b,c,†]

[a] School of Chemical Sciences, National Institute of Science Education and Research (NISER), IOP Campus, P.O. Sainik School, Bhubaneswar 751005, Orissa, India
[b] JC Bose Fellow, Division of Organic Chemistry, National Chemical Laboratory, Pune 411008, India
[c] Indian Institute of Science Education and Research (IISER), 900, NCL Innovation Park, Dr. Homi Bhabha Road, Pune 411008, India

ARTICLE INFO

Article history:
Received 21 June 2010
Received in revised form 24 September 2010
Accepted 27 September 2010
Available online 1 October 2010

Keywords:
DNA, RNA and PNA
A, T, G and C
aep-PNA
Conformational analysis
Pyrrolidine ring

ABSTRACT

The *aep*-PNA is a chiral and cyclic PNA analogue, which has a stronger and base dependent binding affinity with complementary DNA. To understand the base dependent properties at monomer level, the structural studies of *aep*-PNA-(T/C/A) monomers have been carried out focussing on the conformational analysis of pyrrolidine ring pucker in *aep*-PNA by ^{1}H NMR and the coupling constant data fitted into PSEUROT software. The results indicate that the type of pyrrolidine pucker depends on the electronic nature of substituent, implying the effect of pyrimidine or purine substituents in determining the ring pucker in monomers. This may consequently influence the *aep*-PNA oligomer conformation. Since pyrrolidine nucleic acids have emerged as an important class of PNA analogues, present results may have importance for their future development.

1. Introduction

The study of relation between structure and function of biomolecules is very important in understanding the biological functions of living systems.[1] The conformational state of active molecules is a critical factor in determining molecular structure–function relationship. A conformer is not an isolable form of a compound and hence it cannot be analyzed exclusively for biological activity and many times inter-conversion of different conformers is possible. The identification and characterization of conformers depend on the rate of inter-conversion of different conformers and appropriate techniques to detect them in relevant time scale is important.[2] The molecular resolution of interconverting conformers is favoured by lowering the temperature to lessen the rate of inter-conversion and analysis may be done by X-ray crystallography and NMR techniques.[3,4] The X-ray diffraction study provides only the structure of a stable conformer while NMR has the potential to provide information on a mixture of conformers, including the kinetics and thermodynamics of their interconversion.[5] The vicinal proton–proton coupling constants (J) as determined by ^{1}H NMR are weighted averages of the geometry of conformers and by use of Karplus equation aids in determining the stereochemistry of organic molecules, especially the dihedral angle.[6–8] The measured J is also a function of the electronegativity of the substituent and the relationship has been extensively used to find the conformations of the puckered ring in cyclic molecules, wherein fast conformational equilibrium may exist among different puckered states.[9–11] In cyclopentane derivatives, the ring strain is relieved by puckering one atom out of plane leading to *gauche* relation among the vicinal substituents.[12–14] In case of furanose ring of nucleosides, Altona and Sundaraingam have developed a formalism to fit the ^{1}H–^{1}H coupling constants into Karplus equation in order to determine the relative amounts of two conformations in furanose ring.[15,16] They have also extended their method to pyrrolidine rings found in prolines by inclusion of suitable parameters to take into account the electronegativity effects.[9a,17,18] In case of *N*-substituted prolines, it is found from X-ray studies that the five-membered ring prefers to adopt either of the two conformations N (North) and S (South) (Fig. 1) corresponding to C4-*endo* and C3-*endo* forms, respectively.[18c,19,20] However in *C*-substituted prolines this may significantly change depending on the electronegativity of the substituents.

By applying PSEUROT programme developed by Altona et al.,[16] we herein report a conformational analysis of the prolyl ring in aminoethyl prolyl (*aep*) peptide nucleic acid (PNA) monomers having different nucleobases A, C, G and T. *aep*-PNA (Fig. 2) is

* Corresponding author. Tel.: +91 674 230 4094/91 674 230 4130; fax: +91 20 2589 9790; e-mail addresses: nagendra@niser.ac.in (N.K. Sharma), kn.ganesh@iiserpune.ac.in (K.N. Ganesh).
URLs: http://www.niser.ac.in, http://www.iiserpune.ac.in
† Tel.: +91 20 2590 8000; fax: +91 20 2589 9790.

0040-4020/$ – see front matter © 2010 Elsevier Ltd. All rights reserved.
doi:10.1016/j.tet.2010.09.082

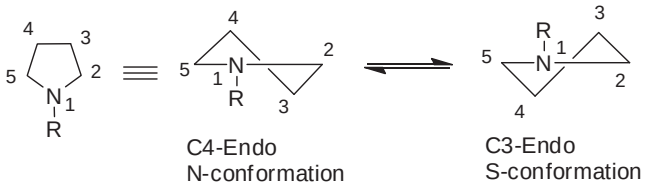

Fig. 1. Conformation of pyrrolidine ring.

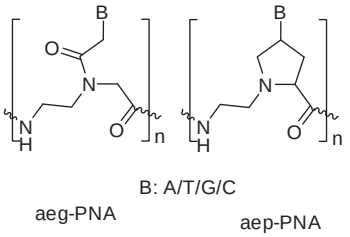

Fig. 2. Structure of *aeg*-PNA and *aep*-PNA.

a conformationally constrained, chiral analogue of the well known acyclic *aeg*-PNA that has shown promising biophysical properties desired for antisense agents.[21] It exhibits base dependent selectivity and affinity to bind complementary DNA sequences. Since the conformation of the prolyl ring may depend on the electronegativity of the substituent, it would be interesting to see whether the attached A, G, C or T nucleobase has any specific effect on the pyrrolidine ring pucker in *aep*-PNA due to their differing group electronegativities and if so, that may explain the observed base dependent specificity effects in *aep*-PNA.

2. Results and discussion

In Scheme 1, the *aep*-PNA derivatives with different substituents on C4 of proline (**2**–**11**) were synthesized from *N*-alkylated 4-hydroxy proline intermediates (**1**) by following our earlier reported procedures.[22] PSEUROT analysis of conformational puckering of five-membered pyrrolidine ring requires measurement of vicinal coupling constants of ring protons and this necessitates an unambiguous assignment their chemical shifts in ^{1}H NMR, which is not always straightforward due to overlapping signals.

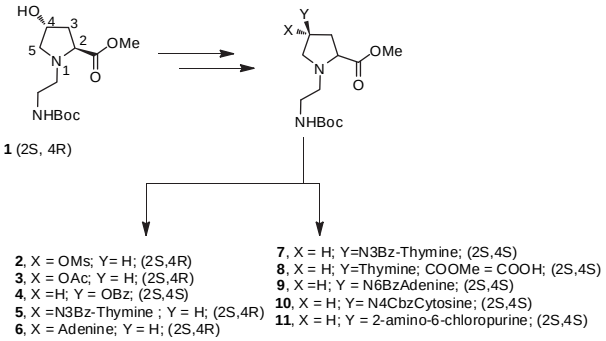

Scheme 1. Synthesis of pyrrolidine derivatives.

2.1. Assignment of pyrrolidine ring protons in *aep*-derivatives

The assignment of common precursor **1** of all target prolyl derivatives including the monomers of *aep*-PNA was done by decoupling methods. The stepwise details of this method are given in SI. The assignment of prolyl ring protons in compound **1** was done by serial decoupling of ^{1}H NMR peaks, which significantly simplified the splitting pattern of vicinal coupling protons. This enabled the identification of the chemical shifts of all prolyl ring protons in compound **1**. The ^{1}H chemical shift assignments of all ring protons in the target *aep* compounds *N*-Boc-(2*S*,4*R*)-*aep*-thymine methyl ester (**5**), *N*-Boc-(2*S*,4*S*)-*aep*-thymine methyl ester (**7**), *N*-Boc-(2*S*,4*S*)-*aep*-thymine acid (**8**), *N*-Boc-(2*S*,4*R*)-*aep*-adenine methyl ester (**6**), *N*-Boc-(2*S*,4*S*)-*aep*-adenine methyl ester (**9**), *N*-Boc-(2*S*,4*S*)-*aep*-cytosine(N^{4Cbz}) methyl ester (**10**) and *N*-Boc-(2*S*,4*S*)-*aep*-2-amino-6-chloropurine methyl ester (**11**) were done by 2D ^{1}H–^{1}H COSY spectroscopy.

A typical 2D NMR assignment of vicinal connectivity by use of ^{1}H–^{1}H COSY is illustrated with compound **7** (*aep*-PNA-T monomer) as an example (Fig. 3). The proton H4 is easily assignable as the most downfield shifted signal (δ 5.2) and its identification triggers the assignment of all connected protons in ring by ^{1}H–^{1}H COSY spectral analyses. The peak for H4 at δ 5.2 shows four cross peaks (1–4) corresponding to its coupling with its two neighbours H5′ and H3′, each having 2 non-equivalent protons (H5′H5″ and H3′H3″). Among these, the relative chemical shift values assists in identifying the upfield components (cross peaks 3 and 4) as due to H3′3″ while the downfield signals at (cross peaks 1 and 2) correspond to H5′5″ protons, thus accounting for the observed set of 4 cross peaks 1 (H4–H5″), 2 (H4–H5′), 3 (H4–H3″) and 4 (H4–H3′). The assignment of H3′3″ paves way for identifying the downfield signal at δ 3.6 due to H2 via H2–H3′ and H2–H3″ cross peaks 5 and 7. This completes the assignment of all ring protons. The assignment of *N*-ethylamino side chain protons Ha′a″, Hb′b″ starts from the easily identifiable NH at δ 5.1, which shows two cross peaks at 3.1 due to Hb′ and Hb″, which in turn is coupled to Ha′a″ via cross peaks 8 (Ha′/Ha″–Hb′ and Ha′/Ha″–Hb″).

The relative stereochemistry of H4 with H3′3″ and H5′5″ was determined from 2D NOESY spectra of compound **7** (see in SI), in which the two observed cross peaks 1 (T-H6,H3′), 2 (T-H6,H5′) and 3 (T-H6,H4) indicate the spatial proximity of thymine H6 with the pyrrolidine ring protons H3′ (cross peak 1, upfield component of H3″) and H5′ (cross peak 2, upfield component of H5″) by virtue of all the three located on the same side of the ring along with H4. In this way this also fixes the conformation of pyrrolidine ring. The protons of other *aep*-monomers (**6**, **8**–**11**) were similarly assigned by a combination of 2D ^{1}H–^{1}H COSY and NOESY spectroscopy. Their spectra are depicted in Supplementary data and the chemical shift values of all assigned protons for compounds **1**–**11** are given in Table 1.

2.1.1. Pyrimidine monomers. In both *aep*-PNA-T (**5**, **7** and **8**) and *aep*-PNA-C(N^{4Cbz}) **10**, signal at δ 8.3 due to H6 shows 3 cross peaks, corresponding to H3′ at δ1.9, H5″ at δ 3.2 and with H4. This suggests that in both *aep*-T and *aep*-C monomers, the pyrrolidine ring system has a conformation wherein H6, H5′, H3′ are on the same face of the ring.

2.1.2. Purine monomers. In the case of *aep*-PNA-N^{6Bz}-adenine **9** and *aep*-PNA-2-amino-6-chloro-purine (**10**) the NOESY spectra (Supplementary data) show weak cross peaks from H8 of adenine to H5″ of pyrrolidine ring indicating a conformation of pyrrolidine in which H8 is on the same face as H5′.

2.2. Coupling constant calculation

After completing the assignments of all protons, by ^{1}H–^{1}H COSY and NOESY experiments, the vicinal coupling constants ($^3J_{Hx-Hy}$) of prolyl ring protons in compounds **1**–**6** and **8** were extracted from their ^{1}H NMR spectra and their values are given Table 2. Apart from ^{1}H NMR, 2D J-resolved NMR spectra were used to extract the accurate vicinal coupling constants for prolyl ring protons for compound **1** as it is the common precursor for all other compounds

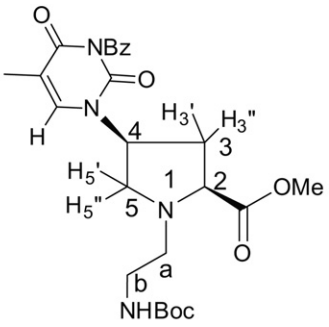

7

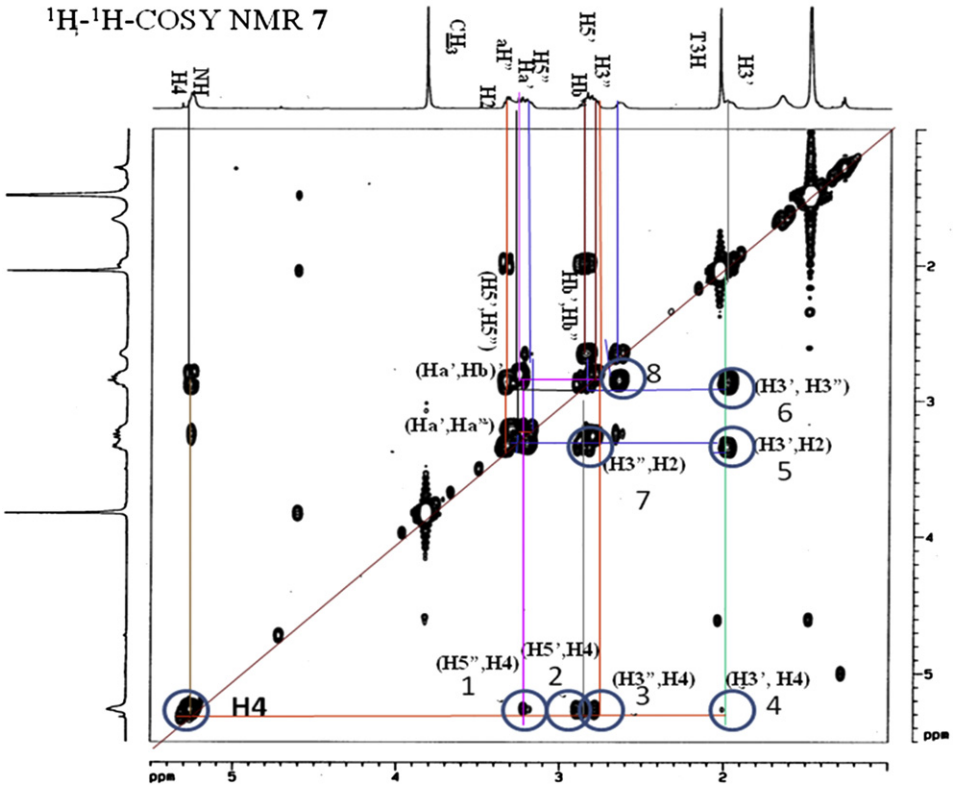

Fig. 3. 2D ^{1}H–^{1}H COSY NMR spectra of pyrrolidine ring protons of compound **7** (500 MHz) in $CDCl_3$. *The numbers 1–7 correspond to cross peaks present in close-by circles.

reported here. A column projections of 2D-J resolved spectra of ring protons of deuterated exchanged compound **1** and its 2D-J resolved spectrum is provided in Supplementary data. We were unable to extract the coupling constants of compounds **7**, **9**, **10** and **11** because of their slight upfield chemical shifts of their H2 protons. As a result, the splitting pattern of proton H2 merged with H5″ and side chain protons b′/b″. The coupling constant values of prolyl ring protons of compounds **1**–**6** and **8** were used as inputs for PSEUROT analysis to deduce the pyrrolidine ring conformations in all compounds.

2.3. Calculation of pyrrolidine ring conformation using PSEUROT 5.4.1

The vicinal coupling constants ($^{3}J_{x-y}$) of ring protons are a function of endocyclic torsion angles. The experimentally measured values were used to derive the pseudorotation phase angle (P), which provides information about the most puckered region of the ring and the puckering amplitude (Φ_m), which indicates the degree of puckering of pyrrolidine rings in various target compounds by using PSEUROT program (version 5.4.1), based on the relation between Φ(H–H) and P as Eq.1:

$$\phi(\mathrm{H{-}H}) = A \times \phi_{\mathrm{Max}} \times \mathrm{Cos}(P + \mathrm{phase}) + B \quad (1)$$

wherein Φ(H–H) is the torsion angle between two vicinal hydrogens and A and B are constants.[15,16] Earlier this programme has been successfully used in the conformational analysis of cyclic ribose and proline derivatives.[18] The torsion angle independent term B has electronegativity dependence and is important in determining the puckering of rings. To determine the conformation of 4-substituted pyrrolidine rings, the values of phase angle P and constant B used as initial input for iterative analysis were as in PSEUROT 5.1.4 software.[16,18]

The primary input parameters for PSEUROT 5.4.1 are the experimentally measured $^{3}J_{H-H}$ in pyrrolidine ring, phase angle P, A and B along with electronegativities values of substituents (see in Supplementary data).[16] The output values obtained from PSEUROT were $^{3}J_{x-y}$ (calculated), P_N (pseudorotation angle for N-conformer), Φ_N, P_S, Φ_s, MF (mole fraction) and dihedral angle (Φ_{Hx-Hy}) of all

Table 1
Chemical shift (ppm) of pyrrolidine ring protons (determined by 1D/2D NMR)[a]

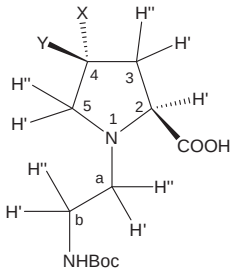

Compound	H2	H3′	H3″	H4	H5′	H5″	aH′	a H″	bH′	bH″	NH	PNA Base Protons
1 (X=OH, Y=H)	3.6	2.2	2.3	4.4	3.4	2.5	2.8	2.8	3.4	3.4	5.3	—
2 (X=OMs, Y=H)	3.6	2.2	2.3	5.3	2.8	3.4	2.6	2.7	3.1	3.1	5.1	—
3 (X=OAc, Y=H)	3.5	2.1	3.3	5.3	2.6	3.5	2.6	2.7	3.1	3.2	5.2	—
4 (X=OBz, Y=H)	3.4	2.2	3.2	4.8	2.7	3.3	2.8	2.8	3.1	3.1	5.4	—
5 (X=N3BzT, Y=H)	3.4	2.2	2.9	4.8	3.8	3.2	2.8	2.8	3.2	3.2	5.2	—
6 (X=A, Y=H)	3.9	2.5	2.5	5.2	3.0	3.9	2.9	2.9	3.2	3.2	5.4	AH8, 8.3, AH2, 7.9
7 (X=H, Y=N3BzT)	3.4	2.0	2.9	5.2	2.8	3.3	2.7	2.9	2.7	2.8	5.2	TH6, 8.1
8 (X=H,Y=T)	4.0	2.3	3.0	**Ov**[a]	3.6	4.0	3.1	3.3	3.1	3.5	**Ex**[a]	TH6, 7.4
9 (X=H,Y=N6BzA)	3.4	2.2	3.0	5.4	3.1	3.4	2.8	2.9	3.2	3.3	5.2	AH8, 8.8, AH2, 8.7
10 (X=H,Y=N4CbzC)	3.4	2.0	2.8	5.3	2.8	3.2	2.6	2.9	3.2	3.3	5.2	CH5, 7.5, CH6, 8.5
11 (X=H, Y=2-amino-6-chloropurine)	3.5	2.2	2.9	5.2	3.0	3.3	2.7	2.9	2.9	3.2	5.3	2-Amino-6-chloropurine 8, 8.3

[a] NMR of all compounds have recorded at 500 MHz NMR in $CDCl_3$ (except acid compound **8** in D_2O). **Ov**: overlapped with D_2O. **Ex**: exchanged with D_2O.

Table 2
Vicinal proton–proton coupling constants (*J*)(Hz)

Compound ($CDCl_3$ /D_2O)	H2-H3′	H2-H3″	H3′-H4	H3″-H4	H4-H5′	H4-H5″
1	7.80	7.80	5.40	5.40	3.40	4.90
2	7.30	7.40	6.80	3.20	2.80	5.50
3	7.30	8.30	3.20	5.90	3.20	6.00
4	6.40	5.80	3.90	4.90	2.00	4.90
5	8.10	7.90	2.90	4.20	3.70	2.90
[a]**6**	6.30	6.50	7.10	5.80	5.90	5.30
[a]**8** (D_2O)	8.10	7.30	5.80	5.90	8.80	3.75

[a] *J* data for compounds **6** and **8** that these are approximate due to overlap of peaks.

vicinal pairs of pyrrolidine ring protons for the two most probable conformers and are shown in Table 3. The validity of PSEUROT is reflected in the difference between J_{exp} and J_{calcd} (ΔJ, Hz), which was in the range 0.0±0.8 Hz corresponding to least root mean square (rms) in range of 0.0–0.5.[9a,17] The mole fraction (MF) of the two probable conformers of pyrrolidine ring MF_N (*N*-conformer; P=0°) and MF_S (*S*-conformer, P=180°) in equilibrium for compounds **1**–**6** and **8** were obtained from the analysis and are shown in Table 3. The dihedral angles Φ_{Hx-Hy} of 4-substituted pyrrolidine ring in compounds **1**–**6** and **8** as computed from PSEUROT analysis are given in Supplementary data.

It is seen from the data in Table 3 that for compounds **1** and **2** (4*R*-hydroxyproline and 4-*O*-mesylproline), *N*- and *S*-conformers are present in almost equal amounts, while for ester compounds **3** and **4** (4-*O*-acetylproline and 4-*O*-benzoylproline), the population of *N*-conformer increases to 75%. In case of *aep*-PNA-T derivatives **5** and **8**, the proportion of *N*-conformer further increases to about 90%. In contrast, for the purine analogue *aep*-PNA-A **6**, the extent of *S*-conformer (55%) slightly increases relative to *N*-conformer, which becomes the minor component. This is also reflected in the values of dihedral angles Φ_N, that is, in the range 44°–68° for the predominant *N*-conformer and decreases to 28° when *S*-conformer predominates.

2.4. Pseudorotation cycle of 4-substituted pyrrolidine derivatives

The pseudorotation cycle of *N*-substituted pyrrolidine derivatives (Fig. 4) is derived from the pseudorotation angle P_N and P_S

Table 3
Geometry of pyrrolidine derivatives from PSEUROT 5.4.1 program

Entry	Compound	MF_N (MF_S)	P_N (P_S)	Φ_N (Φ_S)	rms	Geometrical Symbol of Conformer	Geometry of *N*-conformer (Geometry of *S*-conformer)
1	**1**	0.548	15.2	44.0	0.008	$^4_3$T	C4-*endo* and C3-*exo*
2		(0.452)	(240.0)	(84.4)		(^{5}E)	(C5-*endo* Envelope)
3	**2**	0.503	7.7	59.7	0.216	$^4_3$T	C4-*endo* and C3-*exo*)
4		(0.497)	(229.6)	(82.1)		(^{5}E)	(C5-*endo* Envelope)
5	**3**	0.714	3.9	44.5	0.169	$^4_3$T	C4-*endo* and C3-*exo*
6		(0.286)	(219.6)	(32.7)		($^5_4$T)	(C5-*endo* and C4-*exo*)
7	**4**	0.756	40.3	55.2	0.448	$^4_5$T	C4-*endo* and C5-*exo*
8		(0.244)	(233.4)	(64.7)		(^{5}E)	(C5-*endo* Envelope)
9	**5**	0.934	36.2	68.9	0.112	$^4_5$T	C4-*endo* and C5-*exo*
10		(0.066)	(204.9)	(85.9)		($_4$E)	(C4-*exo* Envelope)
11	**6**	0.449	2.2	68.5	0.279	$^4_3$T	C4-*endo* and C3-*exo*
12		(0.551)	(203.0)	(28.1)		($_4$E)	(C4-*endo* Envelope)
13	**8**	0.857	41.9	68.4	0.180	$^4_5$T	C4-*endo* and C5-*exo*
14		(0.143)	(204.9)	(85.9)		($_4$E)	(C4-*exo* Envelope)

MF_1: mole fraction of type I conformer; MF_2: mole fraction of type II conformer; P_1 and P_2 are pseudorotation angle of type I and type II conformer; Φ_N and Φ_S are amplitude of *N*-type conformer and *S*-type conformer; T: twist form of pyrrolidine; E: envelope form of pyrrolidine.

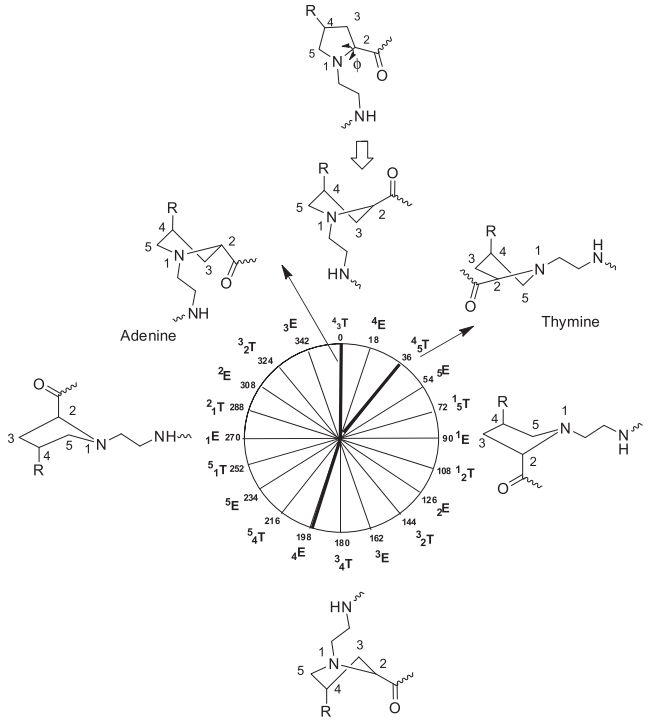

Fig. 4. Pseudorotation cycle for *N*-substituted pyrrolidines.

analogous to that of the furanose and pyrrolidine ring.[7,18,23] When the data of Table 3 are fitted into the pseudorotational cycle, the geometry of pyrrolidine ring corresponds to C4-*endo*/C3-*exo* ($^4_3$T) for both 4-OH and 4-*O*-substituted pyrrolidines. In comparison, the pyrrolidine ring in 4*S*-*O*-benzoyl pyrrolidine **4** with P_N=36.2°, 4*R*-N3Bz-thyminyl pyrrolidine **5** with P_N=40.3° and 4*S*-thyminyl pyrrolidine **6** with P_N=41.9° correspond to C4-*endo*/C5-*exo* ($^4_5$T) geometry (Table 3, entry 13, and Fig. 4). For 4*R*-adeninyl pyrrolidine **7**, the envelope form C4-*exo* ($_4$E) geometry is observed with P_S=28.1° for the major conformer. Thus from the pseudorotation angle computed from the PSEUROT analysis, the geometry of pyrrolidine ring of 4-substituted compounds **1**–**8** may attributed to C4-*endo*/C3-*exo* ($^4_3$T), C4-*endo*/C5-*exo* ($^4_5$T) or C4-*exo* envelope ($_4$E).

The results indicate that the nature of the 4-substituent on pyrrolidine ring to play a significant role in defining the pucker of the pyrrolidine ring in *aep*-PNA and its derivatives. Since purine or pyrimidine nucleobases, certainly differ in terms of their electron withdrawing capacity, their substitution on the pyrrolidine ring in

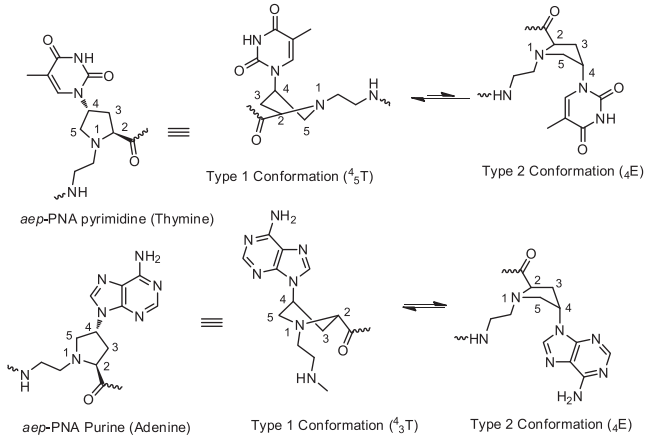

Fig. 5. The most probable conformation of pyrrolidine ring in *aep*-PNA.

aep-PNA would lead to differential ring puckering as clearly suggested by present results. The preferred purine($^4_3$T)/pyrimidine ($^4_5$T) conformational puckering (Fig. 5) as seen in monomers would consequently lead to base dependent variation in the PNA oligomeric backbone.

3. Conclusions

We have herein demonstrated a method to deduce the probable major conformation of pyrrolidine ring in different *aep*-PNA monomers by experimental measurement of the vicinal ^{1}H–^{1}H coupling constants and fitting them into PSEUROT analysis. The ^{1}H NMR spectra were assigned by 2D-COSY/NOESY NMR spectroscopy. 2D J-resolved spectra enabled the measurement of coupling constants, which were used as inputs into the PSEUROT program of Altona et al.[16] to delineate the equilibrium conformations adopted by 4-substituted pyrrolidine rings. It was seen that in 4-*O*-substituted pyrrolidines, the *N*-conformer was preferred in solution. When C4 of the pyrrolidine ring carries a pyrimidine substitution (T or C^{N4CBZ}), the conformation of ring is remarkably biased to *N*-type (85–93%) and for purine-substituted pyrrolidines (A) the conformational equilibrium is slightly shifted to the *S*-conformer (55.1%). This is similar to the observations of Altona and Sundaralingam[5a,24] for the deoxyribose and ribose rings in nucleotides, which also exhibit a slight conformational preference for *S*-type for purine ribosides and *N*-type conformation for pyrimidines. The observed pyrrolidine pucker in *aep*-PNA monomers is thus purine/pyrimidine base dependent with $^4_5$T conformation of pyrrolidine preferred in *aep*-PNA-T and C, while $_4$E preferred in *aep*-PNA-A. This conformational bias in *aep*-PNA monomers may have a cumulative influence on the conformation of different base substituted oligomeric backbone with consequence in influencing the final hybridization properties of the derived *aep*-PNA oligomers.

Acknowledgements

NKS thanks to CSIR-UGC and NCL for giving opportunity to carry out work. We acknowledge the assistance of Dr. P. Rajmohanan in NMR-analysis. We thank to Prof. C. Altona for a generous gift of PSEUROT 5.1.4 software program. We also thank to NISER-Department of Atomic Energy, Govt. of India for continuing my research work.

Supplementary data

2D-NMR of all compounds, electronegativity value of pyrrolidine substituents, input and output data of compounds **1**–**6**, **8** are given in Supplementary data. PSEUROT data of these compounds are depicted in Supplementary data. Supplementary data associated with this article can be found in the online version, at doi:10.1016/j.tet.2010.09.082. These data include MOL files and InChIKeys of the most important compounds described in this article.

References and notes

1. (a) Franchetti, P.; Marchetti, S.; Cappellacci, L.; Jayaram, H. N.; Yalowitz, J. A.; Goldstein, B. M.; Barascut, J. L.; Dukhan, D.; Imbach, J. L.; Grifantini, M. *J. Med. Chem.* **2000**, *43*, 1264–1270; (b) Seela, F.; Peng, X. *J. Org. Chem.* **2006**, *71*, 81–90.
2. (a) Podkorytov, I. S.; Skrynnikov, N. R. *J. Magn. Reson.* **2004**, *169*, 164–173; (b) Maag, H.; Nelson, J. T.; Steiner, J. L.; Prisbe, E. J. *J. Med. Chem.* **1994**, *37*, 431–438.
3. David, W. I. F.; Ibberson, R. M. *Acta Crystallogr., Sect. C* **1992**, *48*, 301–303.
4. (a) Cardenas, F.; Caba, J. M.; Feliz, M.; Lloyd-Williams, P.; Giralt, E. *J. Org. Chem.* **2003**, *68*, 9554–9562; (b) Mac Arthur, M. W.; Thornton, J. M. *Protein* **1993**, *17*, 232–251.
5. (a) Barchi, J. J., Jr.; Karki, R. G.; Nicklaus, M. C.; Siddiqui, M. A.; George, C.; Mikhailopulo, I. A.; Marquez, V. E. *J. Am. Chem. Soc.* **2008**, *130*, 9048–9057; (b) van den Hoogen, Y. T.; Hilgersom, C. M.; Brozda, D.; Lesiak, K.; Torrence, P. F.; Altona, C. *Eur. J. Biochem.* **1989**, *182*, 629–637.
6. (a) Karplus, M.; Anderson, D. H. *J. Chem. Phys.* **1959**, *30*, 6–10; (b) Karplus, M. *J. Chem. Phys.* **1959**, *30*, 11–15.

7. Wu, A. A.; Cremer, D.; Auer, A. A.; Gauss, J. *J. Phys. Chem. A* **2002**, *106*, 657–667.
8. (a) Ludvigsen, S.; Andersen, K. V.; Poulsen, F. M. *J. Mol. Biol.* **1991**, *217*, 731–736; (b) Mikhailopulo, I. A.; Pricota, T. I.; Sivets, G. G.; Altona, C. *J. Org. Chem.* **2003**, *68*, 5897–5908.
9. (a) Haasnoot, C. A. G.; De Leeuw, F. A. A. M.; Altona, C. *Tetrahedron* **1980**, *36*, 2783–2792; (b) Barchi, J. J., Jr.; Jeong, L. S.; Siddiqui, M. A.; Marquez, V. E. *J. Biochem. Biophys. Methods* **1997**, *34*, 11–29.
10. Diez, E.; Palma, J.; San-Fabian, J.; Guilleme, J. *J. Comput. Chem.* **1988**, *9*, 189–199.
11. Pachler, K. G. R. *Tetrahedron* **1971**, *27*, 187–199.
12. Kutzelnigg, W.; Fleischer, U.; Schindler, M. *In NMR-Basic Principles and Progress*; Springer: Heidelberg, 1990; 23; 165–168.
13. Wu, A.; Cremer, D. *Int. J. Mol. Sci.* **2003**, *4*, 158–192.
14. Cremer, D. *J. Phys. Chem.* **1990**, *94*, 5502–5509.
15. (a) Oppenheimer, N. J.; Kaplan, N. O. *Biochemistry* **1976**, *15*, 3981–3988; (b) Guschlbauer, W. *Biochim. Biophys. Acta* **1980**, *610*, 47–55.
16. (a) Altona, C.; Sundaralingam, M. *J. Am. Chem. Soc.* **1972**, *94*, 8205–8212; (b) Altona, C.; Sundaralingam, M. *J. Am. Chem. Soc.* **1973**, *95*, 2333–2344; (c) Hendrickx, P. M.; Martins, J. C. *Chem. Cent. J.* **2008**, *2*: 20 (1–7).
17. Haasnoot, C. A. G.; de Leeuw, F. A. A. M.; de Leeuw, H. P. M.; Altona, C. *Biopolymers* **1981**, *20*, 1211–1245.
18. (a) Deleeuw, F.; Altona, C. *J. Comput. Chem.* **1983**, *4*, 428–437; Westhof, E.; Sundaralingam, M. *J. Am. Chem. Soc.* **1983**, *105*, 970–976; (b) Thibaudeau, C.; Plavec, J.; Carg, N.; Papchikhin, A.; Chattopadhyaya, J. *J. Am. Chem. Soc.* **1994**, *116*, 4038–4043; (c) Houseknecht, J. B.; Altona, C.; Hadad, C. M.; Lowary, T. L. *J. Org. Chem.* **2002**, *67*, 4647–4651.
19. De Leeuw, H. P. M.; Haasnoot, C. A. G.; Altona, C. *Isr. J. Chem.* **1980**, *20*, 108–126.
20. Kilpatrick, J. E.; Pitzer, K. S.; Spitzer, R. *J. Am. Chem. Soc.* **1947**, *69*, 2483.
21. (a) Ganesh, K. N.; Nielsen, P. E. *Curr. Org. Chem.* **2000**, 931–943; (b) Kumar, V. A.; Ganesh, K. N. *Acc. Chem. Res.* **2005**, *38*, 404–412.
22. (a) D'Costa, M.; Kumar, V. A.; Ganesh, K. N. *Org. Lett.* **1999**, *1*, 513–1516; (b) D'Costa, M.; Kumar, V. A.; Ganesh, K. N. *Org. Lett.* **2001**, *3*, 1281–1284; (c) Sharma, N. K.; Ganesh, K. N. *Tetrahedron Lett.* **2004**, *45*, 1403–1406.
23. (a) Han, S. J.; Kang, Y. K. *J. Mol. Struct. (Theochem)* **1996**, *369*, 157–165; (b) Watts, J. K.; Sadalapure, K.; Choubdar, N.; Pinto, B. M.; Damha, M. J. *J. Org. Chem.* **2006**, *71*, 921–925.
24. Haasnoot, C. A. G. *J. Am. Chem. Soc.* **1993**, *115*, 1460–1468.